



## Parameters Affecting Synthesis of Sulfonated Chitosan Membrane for Proton Exchange Membrane in Fuel Cells

Sara G. Abd-elnaeem,<sup>a\*</sup> Azza.I.Hafez,<sup>a</sup> Kamel M. El-khatib,<sup>a</sup> Heba Abdallah,<sup>a</sup> M K Fouad,<sup>b</sup> E.F. Abadir<sup>b</sup>

<sup>a</sup> Chemical Engineering and Pilot Plant Department, Engineering and Renewable Energy Research Institute, National Research Center, Egypt

<sup>b</sup> Chemical Engineering Department, Faculty of Engineering, Cairo University, Egypt



### Abstract

Sulfonated chitosan (SCS) was prepared and characterized to be used in the preparation of poly electrolyte membranes in fuel cells (PEMFCs). The studied parameters were: sulfonating agents and their concentrations; reaction time; temperatures; and stirring rates. The characterizations of chitosan (CS) and SCS were investigated by <sup>1</sup>HNMR, FTIR, XRD, TGA, and DTG. Degree of sulfonation (DS), ionic exchange capacity (IEC), and sulfur content (Sc) of SCS were 71.256%, 0.4502 mmol/g, and 1.447%, respectively, at optimum sulfonating conditions of 12 hr, 70 °C, and 600 rpm by using 4 M sulfuric acid. The water uptake of the SCS membrane was 37.4%, and the mechanical properties were 6.95 MPa and 14% for tensile strength and elongation at break, respectively.

**Keywords:** Chitosan; Sulfonation; Poly electrolyte membrane; Fuel cell; Ion exchange capacity.

### 1. Introduction

Hydrogen is one of the most environmentally benign energy sources that has potential as a fossil fuel alternative. Proton exchange membrane fuel cells (PEMFCs), which produce fewer pollutants, may convert the chemical energy of hydrogen straight into electrical energy. In PEMFCs, which are constructed of stacking components, the membrane electrode assembly (MEA) acts as the heart component. To distinguish between the fuel and oxidant gases, the polyelectrolyte membrane layer in the MEA transmits protons from the anode to the cathode. Prefluoro-sulfonated acids like Nafion and sulfonated engineering polymers now make up the majority of the proton exchange membrane (PEM), also known as the solid polymer electrolyte membrane used in fuel cells (FCs). [1-11] Before fuel cell technology is widely adopted on a commercial scale, Nafion membranes must be able to meet a number of difficulties, including increased performance, lower cost, greater durability, better water management, and the ability to operate at higher temperatures. The potential for PEMs to improve is therefore

considerable [4–6][12-15]. Protons should be successfully conducted by low-cost raw materials, which should serve as the foundation for the development of substitutes for the current commercial fuel cell electrolytes.

Particularly, PEM made from natural polymers is developing into a feasible replacement for currently utilized synthetic polymers because it is affordable and environmentally benign [1-3][7,8,12,13]. CS is one of the numerous inexpensive natural polymers that are also eco-friendly. It is a bio-resource made of polysaccharides produced from chitin. It is distinguished by its exceptional biocompatibility, hydrophobicity (a desirable quality for application in high-temperature environments with low humidity levels), and available functionalities in the CS backbone that enable chemical modification to customize its properties [16-21]. CS has been generating a great deal of interest for a variety of applications. [22- 37] Due to the derivatives of CS, which are created by altering their fundamental structure to produce polymers with a wide range of properties [27, 38], there are numerous approaches to

\*Corresponding author e-mail: [sara.gamil.m@eng-st.cu.edu.eg](mailto:sara.gamil.m@eng-st.cu.edu.eg)

Receive Date: 21 September 2023, Revise Date: 09 November 2023, Accept Date: 13 November 2023

DOI: [10.21608/EJCHEM.2023.230907.8651](https://doi.org/10.21608/EJCHEM.2023.230907.8651)

©2024 National Information and Documentation Center (NIDOC)

use CS. The fact that CS contains three different polar functional groups, including ether (C O C), hydroxyl (OH), and primary amine (NH<sub>2</sub>), contributes to its high water-drawing ability. The OH and NH<sub>2</sub> atoms in CS form functional groups, which allow for a number of chemical modifications to be made to it to suit various needs Fig.1 shows the chemical composition of CS.

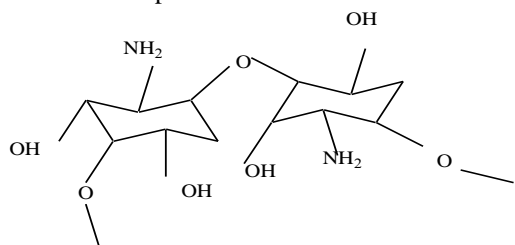


Fig. 1: Chemical structures of chitosan

CS has extremely weak proton conductivity and cannot be used as a PEM in its pure form because its native structure doesn't contain mobile protons. A number of modification methods, including sulfonation, phosphorylation, chemical crosslinking, inorganic particle filling modification, and blending with other polymers, have been used to improve the proton conductivity of CS-based PEMs. [39-45] An important technique for producing hydrophilic polymers that are proton-conductive, frequently insulators, and appropriate for use in electrochemical devices is sulfonation. It entails replacing the hydrogen atom of an organic molecule with a functional group (SO<sub>3</sub>H). Both N-sulfonated CS and O-sulfonated CS, in which the sulfonate group is linked to the NH<sub>2</sub> sites and the OH sites, respectively, are produced by using sulfonating reagents such as sulfuric acid, chlorosulfonic acid, 1,3-propanol sultone, and others under various reaction conditions [46-50]. A specific density of sulfonate groups can be added to the CS backbone by varying the reaction duration, temperature, and reactant concentration. Ion exchange capacity (IEC) values, which measure the amount of sulfonic acid groups in a material, have a significant impact on a material's proton conductivity. IEC-valued sulfonated polymers typically have strong proton conductivities. Fig. 2 shows the chemical composition of chitosan that has been ionically cross-linked with a sulfate ion.

The goal of the current work is to create a SCS membrane that is cross-linked with sulfuric acid while controlling the factors that influence the level

of sulfonation. This membrane will be used as the foundation for creating PEM in fuel cells that has good proton conductivity, superior thermal stability and mechanical properties, and appropriate water absorption.

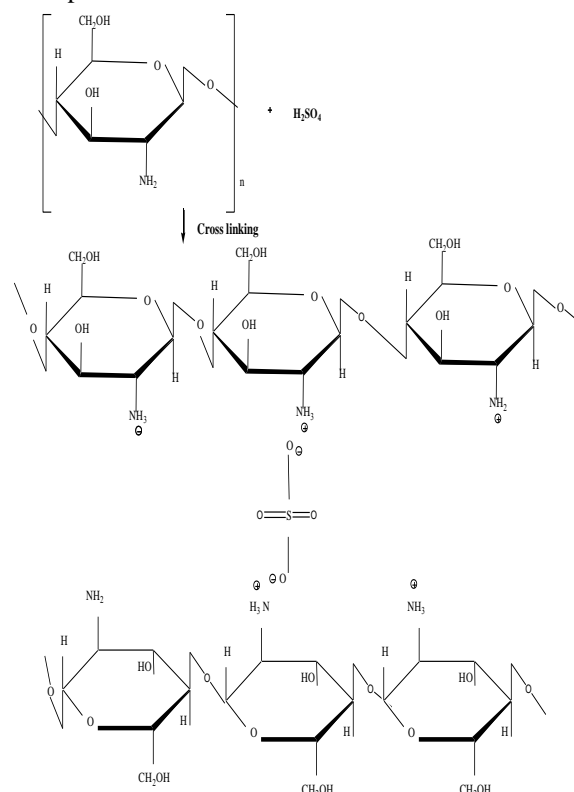


Fig. 2: Chemical structure of ionically cross-linked chitosan with sulfate ion

## 2. Experimental

### 2.1. Chemicals

CS with a molecular weight of 100,000–300,000 was purchased from Acros Organics Company. Sulfuric acid, chlorosulfonic acid, and acetone with a technical grade of 98% were received from Piochem Company. Methanol and ethanol were purchased from Fisher Scientific with a technical grade of 99.8%. Acetic acid and NaOH with technical grades of 99.8% and 98%, respectively, were purchased from Sigma Aldrich Company. 1,3-propane sultone with a technical grade of 97% was purchased from Thermo Scientific Company.

### 2.2. Experimental procedure

#### 2.2.1. Experimental Set up

The experimental set-up used for the preparation of CS powder and SCS membrane is shown in Fig. 3. It consists of a hot plate equipped with a magnetic stirrer and three-neck round bottom flask. One of the

necks is equipped with a condenser for refluxing evaporated vapor; the second neck is used for mixing reactant mixtures by using an ultrasonic stirrer or mechanical stirrer; and the third neck is used for taking samples during reaction.

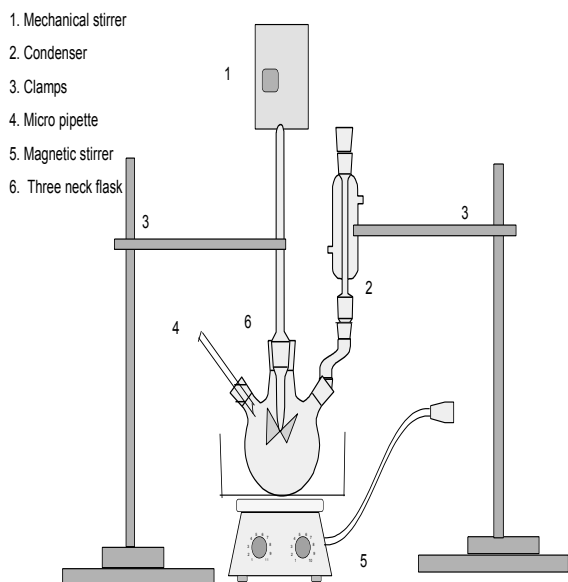


Fig. 3: Experimental set-up of CS sulfonation

#### 2.2.2. Preparation of sulfonated chitosan powder

Water and the majority of organic and alkaline solvents cannot dissolve CS. However, it is dispersible in weak organic acids like formic, lactic, and acetic acids. Acetic acid was the appropriate solvent for CS in the current work. In 500 milliliters of a 1% acetic acid solution, five grams of CS are dissolved using a mechanical stirrer. At various temperatures, times, and stirring speeds, the acid is introduced drop by drop. The procedure is completed by adding the solution to anhydrous ethanol and letting it sit for the night. The solution is neutralized with NaOH to remove any remaining acid, which results in the formation of a white precipitate, then cleaned with acetone and methanol, respectively, followed by drying at 60 °C before the SCS powder is characterized. [51, 52]

#### 2.2.3. Preparation of sulfonated chitosan membrane

One gram of powder SCS is dissolved in 100 ml of formic acid with an ultrasonic stirrer. After complete dissolution of the SCS, the solution will be filtered, cast on a petri dish, and dried for 24 hr at 40 °C [53, 54]. The dried membrane was then neutralized in 2M NaOH for 24 hr before being carefully cleaned. The neutralized SCS membrane

will be next cross-linked for 24 hr using 0.5 M sulfuric acid solution, and then completely rinsed with deionized water in order to eliminate any leftover sulfuric acid. Finally, the SCS membranes will be dried under vacuum for 24 hr at 25 °C. The effect of stirring speed, sulfonation temperature, and time on the degree of sulfonation is investigated to arrive at the optimum condition of CS sulfonation.

### 3.3. Characterizations

#### 3.1. Nuclear Magnetic Resonance Spectra (<sup>1</sup>H NMR)

A <sup>1</sup>H NMR spectrometer (300 MHz, JEOL) will be used for the determination of the DS of SCS. Trifluorofluorine (TFF) and dimethyl sulfoxide (DMSO) were employed as standard solutions for dissolving the tested samples. Integrating the various aromatic signals from the <sup>1</sup>H NMR spectrum data allowed us to calculate the DS.

#### 3.2. Determination of ion exchange capacity (IEC) and sulfur content (Sc)

The value of DS obtained from <sup>1</sup>H NMR was used to determine the IEC by using Eq. 1: [55]

$$DS = \frac{IEC * M_{CS}}{1 - (IEC * MW_{SO_3H})} \dots \dots \dots (1)$$

where MCS and MW<sub>SO<sub>3</sub>H</sub> are the molecular weights of CS and SO<sub>3</sub>H, respectively.

The percentage of sulfur (Sc) in the dry sample of SCS was calculated using Eq. 2. [56]

$$IEC = \frac{1000 * S_c}{MW_s} \dots \dots \dots (2)$$

where Sc is the sulfur content (%) and MW<sub>s</sub> is the molecular weight of sulfur.

#### 3.3. X-Ray Diffraction Spectroscopy (XRD)

XRD patterns of CS and SCS are obtained using an X-ray diffractometer (Bruker D8 advance). To investigate the solid state morphology for identifying the changes in the crystal structure, the angles of 0° and 80° were selected for beginning and end, respectively.

#### 3.4. Fourier Transform Infrared (FTIR)

FTIR is measured using Bruker vertex 80 to verify the main functional groups of the CS and SCS with a resolution of 4 cm<sup>-1</sup> and a refractive index of 2.4, in the range of 400–4000 cm<sup>-1</sup>.

### 3.5. Scanning electron microscopy (SEM)

SEM enables the visualization of the surface and cross-sectional morphologies of the CS and SCS samples by using various magnifications. Images were captured using a JEOL 5410 SEM operating at 20 kV.

### 3.6. Thermal Analysis

The thermal characteristics of CS and SCS are determined using thermal gravimetric analysis (TGA). A relative value of the original mass (%) can be used to indicate the mass change, or TGA. When stated as (%/min), DTG is a differentiation of TGA over time. The TGA and DTG curves for the CS and SCS samples are obtained using the Themys One+ device. The temperatures are employed between 30 and 200 °C, with a 10 °C/min heating rate, and carrier gas nitrogen is used with a flowing rate of 50 ml/min.

### 3.7. Water uptake measurements

In deionized water, the prepared SCS membrane was submerged and left to soak for 24 hr. After being taken out of the water, the film was quickly dabbed with filter paper to remove any leftover surface moisture before being weighed (M2). The membrane was dried and weighted (M1). The water absorbed percentage was determined using Eq. 3 [57]:

$$\text{Water uptake (\%)} = \frac{M_2 - M_1}{M_2} * 100 \dots \dots \dots (3)$$

### 3.8. Mechanical properties

The prepared SCS membrane mechanical properties were investigated in order to show how the sulfonation of CS affected those qualities, which were primarily assessed by a tensile test. Using a mechanical testing instrument (INSTRON-5500R) with a measurement accuracy of 5%, the tensile strength and elongation of the membrane were assessed.

## 4. Results and discussions

The SO<sub>3</sub>H group develops the membrane hydrophilic domain, which gives it the capacity to absorb water due to its affinity for water molecules. Thus, this alters the acid's functionality and makes proton transport easier [58, 59]. As a result, since it determines both the membrane conductivity and its mechanical properties, ion exchange capacity measurement is a crucial factor in the synthesis of PEM [60].

### 4.1. Parameters effecting the preparation of sulfonated chitosan (SCS)

Twenty-three experiments were used to specify the optimum operating conditions for sulfonation of CS: sulfonating agents, concentration of sulfonating agents, reaction time, stirring speed (rpm) and reaction temperature.

#### 4.1.1. Choice of suitable sulfonating agents

Three sulfonating agents, namely sulfuric acid, 1,3-propane sultone, and chlorosulfonic acid at a 4 M concentration, were tested. Table 1 presents the effect of the sulfonating agents on SCS formation with respect to their DS, IEC, and Sc at 4M acid concentration, for a reaction time of 3 hr, at 50 °C, and a stirring rate of 400 rpm. It is remarkable that the results showed that the CS has affinity for the entire sulfonating agents (as confirmed with <sup>1</sup>HNMR) with varying DS, IEC, and Sc. Sulfuric acid showed slightly lower values of DS, IEC, and Sc by nearly 1-2% than the other two acids. This may be due to the hydrolytic de-sulfonating effect normally associated with sulfuric acid, as reported in the literature [61, 62]. In addition, the price of sulfuric acid is much lower than that of both other acids; for that reason, it is suitable to use sulfuric acid for the preparation of the SCS.

Table 1: Results of degree of sulfonation, ion exchange capacity, and sulfur content analysis for 4M of different acid concentrations at 50 °C, 3 hr, and a stirring rate of 400 rpm

	4M sulfuric acid	4M 1,3 propane sultone	4M Chlorosulfonic acid
DS%	32.64	36.09	37.315
IEC (mmol/g)	0.2104	0.2322	0.2399
Sc%	0.6732	0.7431	0.7678

#### 4.1.2. Effect of acid concentration on preparation of SCS

Experiments were carried out by using three concentrations of the recommended sulfuric acid for a reaction time of 3 hr, at 50 °C, and a stirring rate of 400 rpm. Fig. 4 demonstrated that the IEC of the resultant SCS is proportional to the DS (the acid groups contained in the polymer matrix). Table 2 concluded that the DS, IEC, and Sc increased as the sulfuric acid concentration increased. Since IEC is dependent on acid concentration, as the IEC rises, more SO<sub>3</sub>H groups should become attached to the polymer matrix, increasing the polymer's hydrophilicity and promoting proton mobility and conductivity of the membrane, as confirmed by

Table 2: Results of DS, IEC, and Sc at varying concentrations of sulfuric acid

Conc	0.5M	2M	4M
DS%	10.145	17.92	32.64
IEC (mmol/g)	0.0679	0.1164	0.2104
Sc%	0.2173	0.3725	0.6732

#### 4.1.3. Effect of time on preparation of SCS

The DS, IEC, and Sc of SCS for various sulfonation times (3–24 hr), at constant CS weight, and at the predetermined conditions: 4M sulfuric acid at 50 °C reaction temperature and a stirring rate of 400 rpm are presented in Table 3. The results showed that SCS contained sulfur, confirming that sulfuric acid had sulfonated the polymer (CS). Meaning that the quantity of accessible acid groups (DS) and their capacity for dissociation in water play a significant role in determining the conductivity of membranes, which is in good agreement with published data [58]. Fig. 5 depicts the results of the DS and IEC of the SCS as a function of sulfonation time. It is remarkable that DS and IEC increase as time increases from 3 hr to 12 hr, then decrease sharply until 24 hr. For that, it can be concluded that the optimum sulfonation time was 12 hr, in which the highest DS and IEC of 57.82% and 0.3679 mmol/g, respectively, obtained and confirmed by Christopher et al;[65], who reported that CS is unfavorably

Table 3: Results of DS, IEC, and Sc analyses at 4M acid concentration at 50°C, and a stirring rate of 400 rpm

Time (hr)	3	6	9	12	18	24
DS%	32.64	42.46	48.78	57.82	43.25	22.147
IEC(mmol/g)	0.2104	0.2723	0.3118	0.3679	0.2772	0.1435
Sc%	0.6732	0.8713	0.9977	1.1771	0.887	0.4593

published data [63, 64]. The highest concentration value of sulfuric acid is achieved at 4 M.

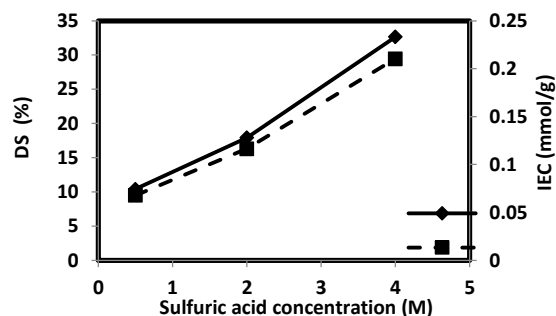


Fig. 4: Effect of different acid concentrations on DS and IEC

affected by extended sulfonation, which could cause the polymer chain to break down and reduce the number of sites available for attachment (for the SO<sub>3</sub>H group), resulting in a decrease in SCS's DS and IEC. Additionally, it has been noted that prolonged sulfonation times can result in significant membrane solubilities, which are bad for fuel cells. For this reason, it is advised to utilize a maximum sulfonation reaction time of 12 hr.

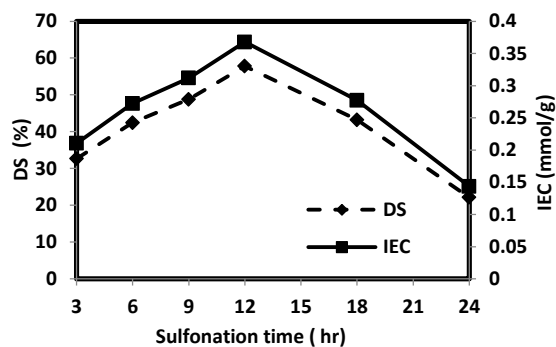


Fig. 5: DS and IEC as a function of reaction time using 4 M sulfuric acid at 50 °C and 400 rpm

#### 4.1.4. Effect of temperatures on preparation of SCS

Between 30 and 70 °C, the impact of temperature on the sulfonation of CS was examined using predetermined conditions: 4 M sulfuric acid for a predetermined time of 12 hr and a stirring rate of 400 rpm. The results for DS, IEC, and Sc are presented in Table 4. As the temperature increased, the DS and IEC increased sharply until 50 °C, then slightly increased to 70 °C. Fig. 6 shows that temperature increases with an increase in the IEC and DS of the resulting CS polymer. At 70 °C, IEC and DS were 0.4217 mmol/g and 66.59%, respectively, compared with IEC of 0.3679 mmol/g and degree of sulfonation of 57.82% at 50 °C. According to this, increasing the temperature of the sulfonation process increases the thermal energy of the system, which in turn speeds up the rate of electrophilic substitution on the aromatic ring [65]. Therefore, it is suggested to increase the polymer's ion exchange capacity as the

rate of electrophilic substitution rises. We can choose 50 °C as a reasonable temperature for SCS because it has also been observed that severe sulfonation can result in high solubility in a water-soluble membrane, which is bad for fuel cells [65].

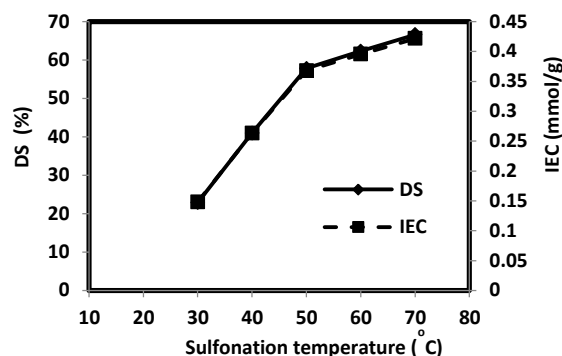


Fig. 6: DS and IEC as a function of temperature at 30, 40, 50, 60, and 70 °C

Table 4: Results of DS, IEC and Sc analysis at 4M acid concentration at 12 hr and stirring rate of 400 rpm

Temp.(°C)	30	40	50	60	70
DS%	22.84	40.99	57.82	62.31	66.59
IEC (mmol/g)	0.1480	0.2631	0.3679	0.3955	0.4217
Sc%	0.4735	0.8418	1.1771	1.2656	1.3496

#### 4.1.5. Effect of stirring speed on preparation of SCS

As it impacts the efficiency of the reaction and the quantity of the product produced, stirring is a crucial component of any chemical process that cannot be disregarded. To better understand the way the sulfonic group transfers mass to the aromatic ring, the influence of stirring speed on the sulfonation of CS was examined. This was done with a 4M sulfuric acid concentration under ideal sulfonation conditions of 12 hr at 70 °C. The five stirring speeds that were investigated were 100, 200, 300, 400, and 600 rpm. Table 5 illustrates how the DS, IEC, and Sc of SCS are affected by the stirring rate. The outcomes demonstrated that stirring speed is a key element in the sulfonation of CS, since DS and IEC rise with increasing stirring speed. The rise in DS and IEC with increasing stirring speed may be caused by an increase in the rate of SO<sub>3</sub>H distribution to the aromatic ring, which, by maintaining uniform SO<sub>3</sub>H group distribution, enables the sulfonation reaction of CS to proceed in the desired direction [65]. From 100 to 400 rpm, DS and IEC increase virtually linearly

and quickly. From 400 to 600 rpm, they climb gradually. We therefore believe that the optimum sulfonation reaction speed is 600 rpm, where the DS%, IEC, and Sc% values are 71.256, 0.4502, and 1.4407, respectively.

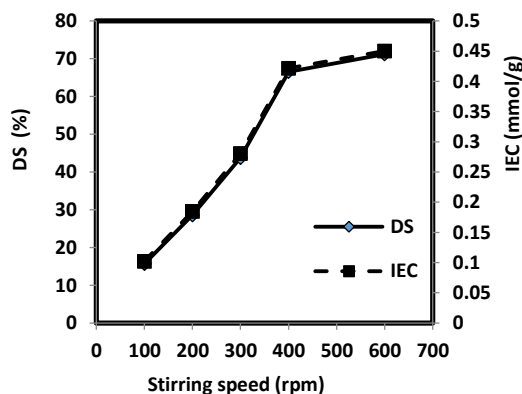


Fig. 7: Effect of stirring speed on sulfonation of CS using 4 M of sulfuric acid, 70 °C, 12 hr.

Table 5: Results of DS, IEC, and Sc analysis at 4M acid concentration at 70°C, 12 hr, and a stirring rate of 400 rpm

Stirring rate, rpm	100	200	300	400	600
DS%	15.7	28.57	43.75	66.59	71.256
IEC (mmol/g)	0.1021	0.1845	0.2804	0.4217	0.4502
Sc%	0.3267	0.5905	0.8972	1.3496	1.4407

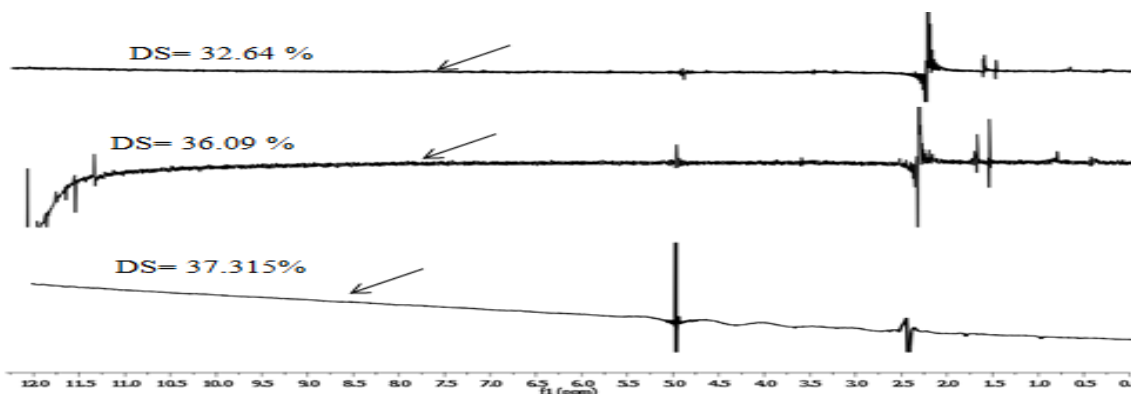
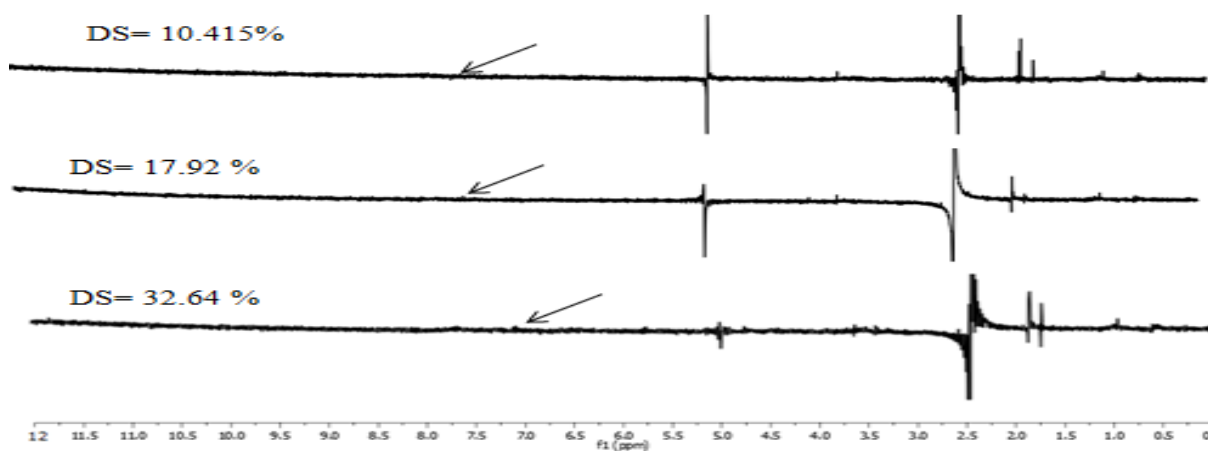
#### 4.1.6. <sup>1</sup>HNMR

The <sup>1</sup>HNMR spectrum of SCS at different operating conditions is shown in Figs. 8–12, indicating that all spectrums showed affinity for SCS at different studied parameters. The humps appearing at 7-9 ppm indicate the presence of sulfonic acid linking in the aromatic ring [65], thus indicating the acid group's effective attachment to the polymer.

#### 4.2. Characterizations of CS and SCS at the optimum conditions

##### 4.2.1. X-ray diffraction (XRD)

As shown in Fig. 13, XRD patterns for CS and SCS have been examined in the 2θ range of 0° to 80°. It is remarkable that two reflections in CS at angles of 2θ = 19° and 2θ = 9° correlate to the crystal structure. The peak for CS at 2θ = 9° moved to 2θ = 15° in SCS, with reduced peak intensity, and the peak intensity of the SCS has also dropped at the position of 2θ = 19°.

Fig. 8: <sup>1</sup>HNMR spectrum of SCS using 4 M sulfuric acid, 1,3- propane sultone, and chlorosulfonic acidFig. 9: <sup>1</sup>HNMR spectrum of SCS using 0.5, 2, and 4M sulfuric

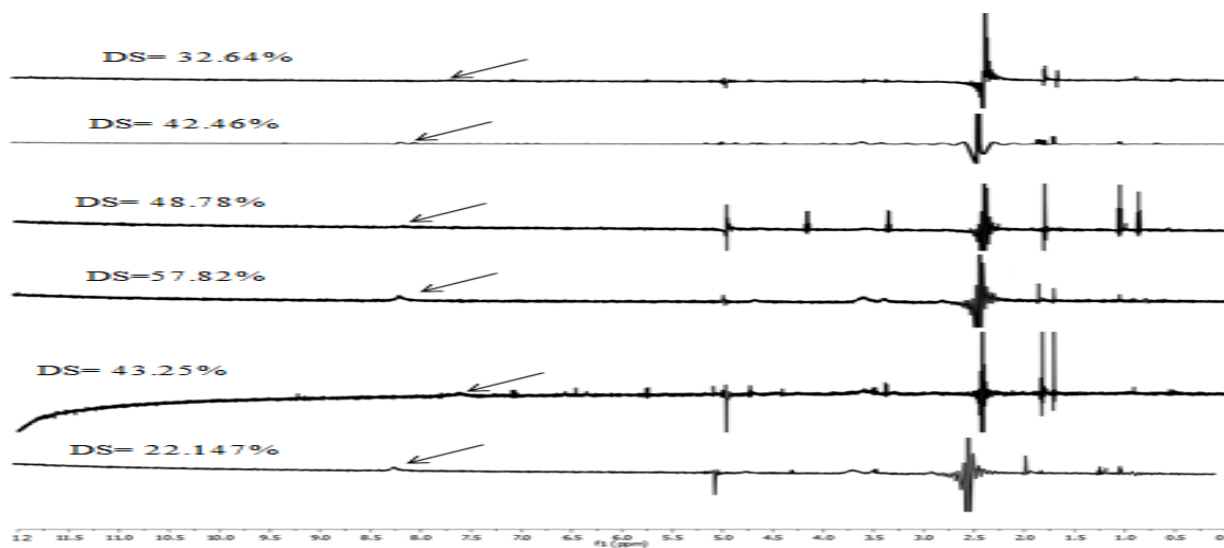


Fig. 10:  $^1\text{H}$ NMR spectrum of SCS using 4 M Sulfuric acid at 3, 6, 9, 12, 18, and 24 hr

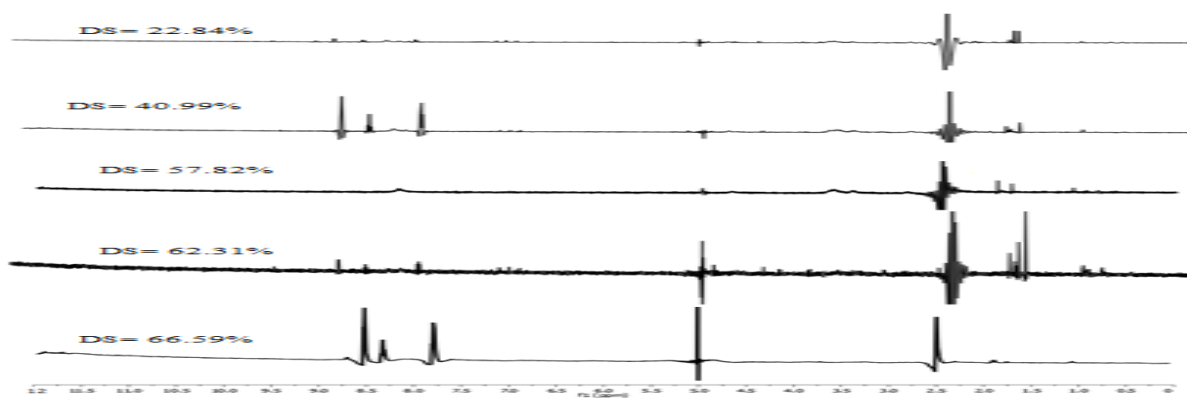


Fig. 11:  $^1\text{H}$ NMR spectrum of SCS using 4 M Sulfuric acid at 30, 40, 50, 60, and 70 °C

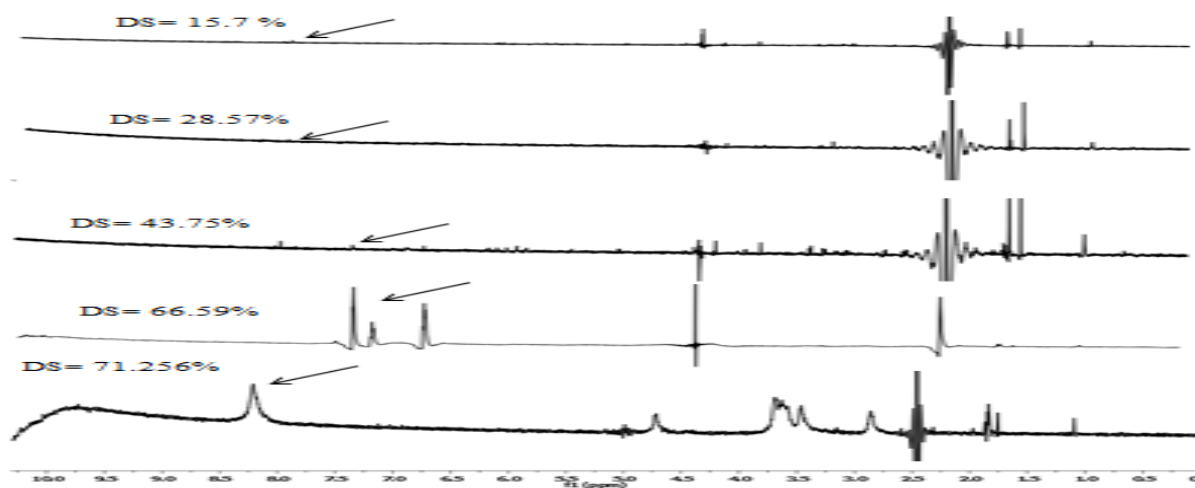


Fig. 12:  $^1\text{H}$ NMR spectrum of sulfonation at stirring rates of 100, 200, 300, 400, and 600 rpm

This may be explained by the fact that the polymer can't absorb more water due to the disordered structure or hydrogen bond loss caused by the sulfonation process. Results were consistent with the previous ones, which demonstrate that after the sulfonation process, the addition of sulfonic groups reduces the crystallinity of CS [35].

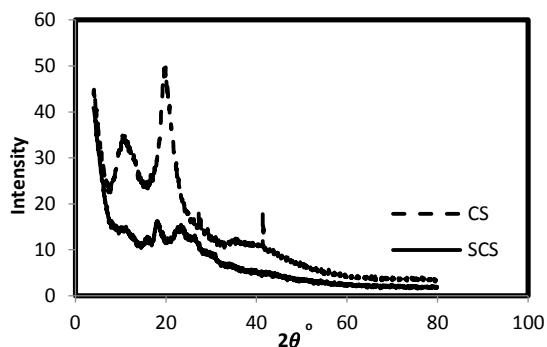


Fig. 13: XRD patterns of CS and SCS

#### 4.2.2. Fourier Transform infrared (FTIR)

The functional groups are identified using FTIR spectroscopy for CS, and SCS is shown in Fig. 14. The CS spectrum observed at  $3360\text{ cm}^{-1}$  is due to O-H stretching, which overlaps with the NH stretching in the same region. The peaks at  $2869\text{ cm}^{-1}$  correspond to  $\text{CH}_2$  stretching. The absorption bands at  $1645$  and  $1585\text{ cm}^{-1}$  could be assigned to the (amide I) and (amide II) bending vibrations. It is obviously seen that the bands at  $1420$  and  $1375\text{ cm}^{-1}$  are due to C-H stretching. The absorption band at  $1320\text{ cm}^{-1}$  could be assigned to the  $-\text{CH}_3$  bend. The peaks at  $1150$ ,  $1061$ , and  $1025\text{ cm}^{-1}$  correspond to C-O-C stretching. While peaks at  $893$  and  $661\text{ cm}^{-1}$  correspond to NH primary and secondary amines. The absorption bands at  $557$ ,  $523$ ,  $453$ ,  $424$ , and  $406\text{ cm}^{-1}$  are due to c-c stretching. Additionally shown in Fig. 14 are the SCS FTIR spectra. It is evident from the peak of Fig. 14 at  $3364\text{ cm}^{-1}$  that it correspond to O-H stretching; the peak at about  $2942\text{ cm}^{-1}$  corresponds to  $\text{CH}_2$  stretching. The peak at  $1628\text{ cm}^{-1}$  corresponds to the bending vibration absorption of the  $\text{NH-SO}_3\text{H}$  group. The peak at  $1525\text{ cm}^{-1}$  which corresponds to the bending vibration of C-N-C, The peak at  $1416\text{ cm}^{-1}$  corresponds to  $\text{NSO}_2$ , and the peak at  $1381\text{ cm}^{-1}$ , which is related to the symmetrical and asymmetrical stretching vibration absorption of sulfate. The peak at about  $1302\text{ cm}^{-1}$  could be assigned to the  $-\text{CH}_3$  bend. The peak at  $1149\text{ cm}^{-1}$

corresponds to C-O-C stretching. Peaks at  $1089$  and  $1017\text{ cm}^{-1}$  are possibly found due to symmetric and asymmetric stretching vibrations of  $\text{S}=\text{O}$  groups. Peaks at  $870$  and  $705\text{ cm}^{-1}$  correspond to  $\text{NSO}_2$ . Peaks at  $575$  and  $431\text{ cm}^{-1}$  correspond to C-C stretching. Peaks were noticed to be sharper in the case of SCS. The modified CS contains sulfonic groups, as shown by all the data above.

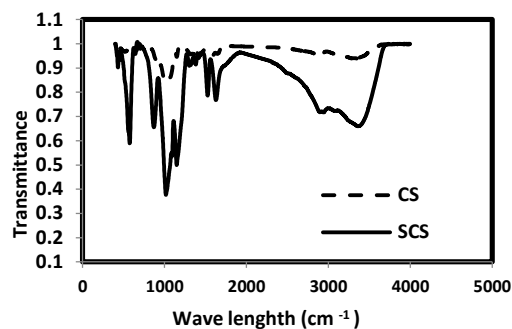


Fig. 14: FTIR spectrum for CS and

#### 4.2.3. Scanning electron microscope (SEM)

The SEM images corresponding to the morphology of CS and optimum SCS are shown in Figs. 15 and 16. In the case of CS, a homogeneous surface free of defects is observed, and no pores exist. The cross-section preparation procedure is mostly responsible for the roughness that is visible in the photos. It is evident from Fig. 16 that the surface of SCS is rougher and more porous than that of CS as it converted from a flat structure to a granular one. The ionic bonds formed by the added sulfonic groups could be the cause of these modifications. [51].

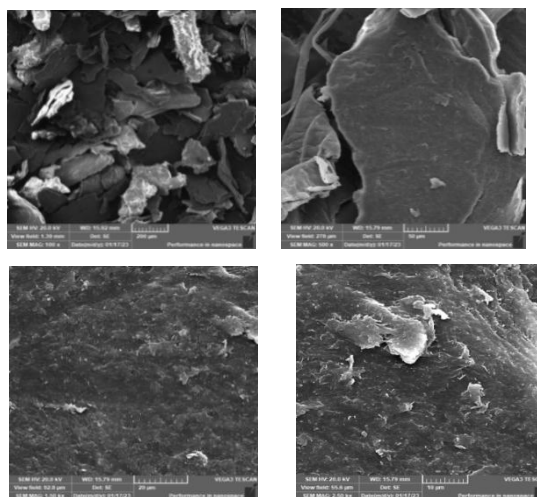


Fig. 15: Scanning electron microscope of CS at different magnifications at 20 KV (X100, X500, X1500 and X2500)

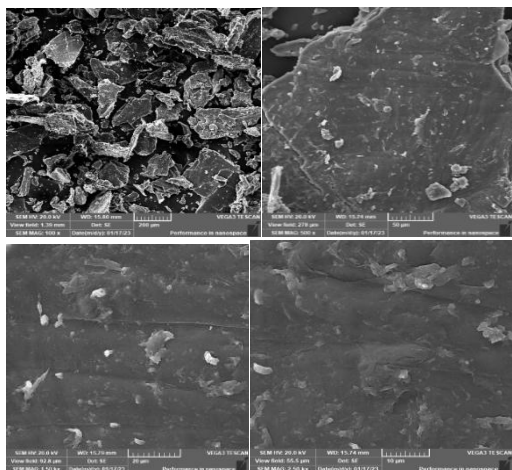


Fig. 16: Scanning electron microscope of SCS at different magnifications at 20 KV (X100, X500, X1500, and X2500)

#### 4.2.4. Thermal Analysis of CS and SCS

Fig. 17 presents the TGA of the CS sample, which was analyzed in nitrogen, showing a three-stage decomposition process. The first stage takes place between 40 and 50 °C with an almost 2% loss of the initial weight. This is followed by a further 4% weight loss just above 50 °C which ends at around 100 °C. The third stage takes place between 100 and 220 °C indicating a weight loss of about 1%. The total weight loss was 7%. The SCS sample analyzed in nitrogen (Fig. 18) shows a four-stage decomposition process. The first stage takes place between 40 and 45 °C with an almost 10% loss of the initial weight. This is followed by a further 20% weight loss just above 45 °C and ends at around 100 °C. The third stage of decomposition, which ends at around 140 °C indicates a weight loss of about 5%. A complete weight loss is attained in the final stage of the sample decomposition, starting at around 140 °C and ending just above 220 °C indicating a weight loss of about 5%. The total weight loss was 40%. Stages between 100 and 220 °C indicate sulfuric acid group degradation; therefore, these outcomes demonstrate the effective incorporation of the sulfonic group into the CS sulfate. [51]. DTG for CS and SCS samples is shown in Fig. 18. The onset of the initial decomposition reaction for CS begins at a lower temperature (83.5 °C) than for SCS (151.4 °C). Furthermore, it can be concluded that SCS polymer is thermally less stable than CS over the full range of the applied temperature [60]. This improvement in thermal stability is related to the high degree of

crosslinking created by the sulfonation reaction, which results in the formation of a network structure with strong sulfonic group crosslinking, and the grafting yield obtained from pure polymers. The sulfonic group has thus been successfully integrated into SCS, as demonstrated by these data.

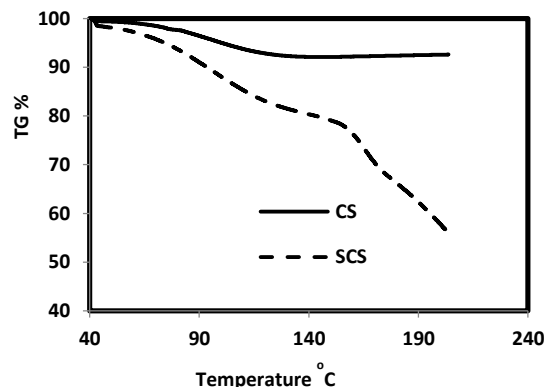


Fig. 17: TGA for CS and SCS

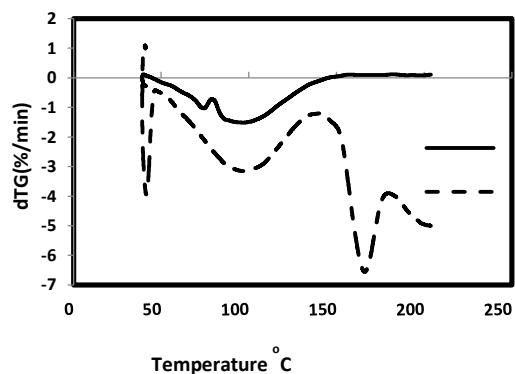


Fig.18: DTG for CS and SCS

#### 4.2.5. Water uptake measurement

Proton carriers, hydrogen bonding networks, and continuous ion transport channels can all be formed in the membrane with the aid of water uptake, which is essential for a PEM's proton conducting efficiency. At 30 °C, the water uptake of SCS was 37.4%, exceeding that of the commercial Nafion 117 membrane, which was only 32% at 30 °C and 34% at 60 °C and 80 °C, respectively. [66]

#### 4.2.6. Mechanical properties

In order to manufacture membrane electrode assemblies and to ensure the durability of the fuel cell while it is operating, a PEM must have favorable mechanical qualities. With a tensile strength and elongation at break of 6.95 MPa and 14%,

respectively, the SCS membrane demonstrated low mechanical stability.

### 5. Conclusions

- The sulfonation technique of CS was utilized to make the biopolymer CS, which is normally an insulator, proton-conductive, and hydrophilic, to be used in electrochemical devices such as fuel cell applications.

- The optimum conditions of CS sulfonation were achieved at 4M sulfuric acid for 70 °C, 12 hr reaction time, and 600 stirring rate, and the DS%, IEC (mmol/g), and Sc% were 256, 0.4502, and 1.4407, respectively.

- The SO<sub>3</sub>H group's attachment to the CS polymer matrix was confirmed by <sup>1</sup>HNMR; the FTIR reveals the presence of sulfonic groups in the SCS; the SEM proved that the surface of SCS was rougher and more porous than that of CS; the XRD demonstrated that the addition of sulfonic groups reduces the crystallinity of CS; and the SCS polymer is thermally less stable than CS over the full range of the applied temperature.

- The water uptake of SCS was 37.4%, which is higher than the commercial Nafion 117, with a tensile strength and an elongation at break of 6.95 MPa and 14%, respectively. The SCS membrane, however, demonstrated low mechanical stability.

### 6. Recommendation

CS provides a low-cost source of SCS membrane, so it is recommended in the future to investigate way to improve SCS mechanical stability and proton conductivity, which are essential for FC applications, by filling out modifications to inorganic particles or by combining them with other polymers. This will also help in the creation of membranes with improved characteristics.

### 7. Conflicts of interest

There are no conflicts to declare.

### 8. Acknowledgment

The authors thank the National Research Centre in Egypt, where this study was conducted, for financial support. In addition, this work was supported by the chemical engineering department, Cairo University.

### 9. References

[1] He, G. W., Nie, L. L., Han, X., Dong, H., Li, Y. F., & Wu, H., Constructing facile proton-conduction pathway within sulfonated poly(ether ether ketone) membrane by incorporating poly(phosphonic acid)/silica nanotubes. *Journal*

of Power Sources, 2014, 259, 203–212. DOI:10.1016/J.JPOWSOUR.2014.02.091

- [2] Park, C. H., Lee, C. H., Guiver, M. D., & Lee, Y. M. Sulfonated hydrocarbon membranes for medium-temperature and low-humidity proton exchange membrane fuel cells (PEMFCs). *Progress in Polymer Science*, 2011, 36, 1443–1498. DOI: 10.1016/j.progpolymsci.2011.06.001
- [3] Wen, S., Gong, C. L., Tsen, W. C., Shu, Y. C., & Tsai, F. C. Sulfonated poly(ether sulfone)/silica composite membranes for direct methanol fuel cells. *Journal of Polymer Science*, 2010, 116, 1491–1498. DOI:10.1002/app.31699
- [4] Badwal SPS, Giddey SS, Munnings C et al, Emerging electrochemical energy conversion and storage technologies. *Front Chem*, 2014, 2:1–28. doi:10.3389/fchem.2014.00079
- [5] Page KA, Rowe BW An overview of polymer electrolyte membranes for fuel cell applications. In: *Polym Energy Storage Deliv Polyelectrolytes Batter Fuel Cells*, American Chemical Society, 2012, pp 147–164. <https://doi.org/10.1021/bk-2012-1096.ch009>
- [6] Savadago O. Emerging membranes for electrochemical systems: (I) solid polymer electrolyte membranes for fuel cell systems. *J New Mater Electrochem Syst* 1998;1:47–66. DOI:10.1002/CHIN.199847334
- [7] ajesh G. Bodkhe, Rakesh L. Shrivastava, Vinod Kumar Soni, Rajkumar B. Chadge, A review of renewable hydrogen generation and proton exchange membrane fuel cell technology for sustainable energy development, *International Journal of Electrochemical Science*, 2023, Volume 18, Issue 5. <https://doi.org/10.1016/j.ijoes.2023.100108>
- [8] Tabbi Wilberforce, Zaki El-Hassan, F.N. Khatib, Ahmed Al Makky, Ahmad Baroutaji, James G. Carton, Abdul G. Olabi, Developments of electric cars and fuel cell hydrogen electric cars, *International Journal of Hydrogen Energy*, 2017, Volume 42, Issue 40, Pages 25695-25734. <https://doi.org/10.1016/j.ijhydene.2017.07.054>
- [9] Abokhalil, A.G., Alobaid, M.; Makky, A.A. Innovative Approaches to Enhance the Performance and Durability of Proton Exchange Membrane Fuel Cells, *Energies*, 2023, 16, 5572. <https://doi.org/10.3390/en16145572>
- [10] Rosli, N.A.H.; Loh, K.S.; Wong, W.Y.; Yunus, R.M.; Lee, T.K.; Ahmad, A.; Chong, S.T. Review of Chitosan-Based Polymers as Proton Exchange Membranes and Roles of Chitosan-Supported Ionic Liquids. *Int. J. Mol. Sci*, 2020, 21, 632. <https://doi.org/10.3390/ijms21020632>
- [11] Tushar Kanti Maiti, Jitendra Singh, Jagannath Majhi, Arihant Ahuja, Subrata Maiti, Prakhay Dixit, Sakchi Bhushan, Anasuya Bandyopadhyay,

- Sujay Chattopadhyay, Advances in polybenzimidazole based membranes for fuel cell applications that overcome Nafion membranes constraints, *Polymer*, 2022, Volume 255. <https://doi.org/10.1016/j.polymer.2022.125151>
- [12] Collier Amanda, Wang Haijiang, Yuan Xiao Zi, Zhang Jiujun, Wilkinson David P. Degradation of polymer electrolyte membranes. *Int J Hydrogen Energy* 2006; 31(13):1838–54. DOI:10.1016/j.ijhydene.2006.05.006
- [13] Bao Cheng, Ouyang Minggao, Yi Baolian. Analysis of the water and thermal management in proton exchange membrane fuel cell systems. *Int J Hydrogen Energy* 2006; 31(8):1040–57. DOI:10.1016/j.ijhydene.2005.12.011
- [14] Parekh Abhi, Recent developments of proton exchange membranes for PEMFC: A review, *Frontiers in Energy Research*, 2022, Volume 10. <https://doi.org/10.3389/fenrg.2022.956132>
- [15] M. F. A. Kamaroddin, N. Sabli, and T. A. T. Abdullah, ‘Hydrogen Production by Membrane Water Splitting Technologies’, *Advances In Hydrogen Generation Technologies*, InTech, 2018, Aug. 22. DOI:10.5772/intechopen.76727
- [16] Musa, M.T., et al., Recent biopolymers used for membrane fuel cells: Characterization analysis perspectives, *International Journal of Energy Research*, 2022, 46(10). <https://doi.org/10.1002/er.8329>
- [17] Saiqa Ikram, Shakeel Ahmed, S. Wazed Ali, Himanshu Agarwal “Chitosan-Based Polymer Electrolyte Membranes for Fuel cell applications”, *Organic-Inorganic Composite Polymer Electrolyte Membranes J.* 2017, pp. 381-398. DOI:10.1007/978-3-319-52739-0\_15
- [18] Lupatini, K.N., et al., Development of Chitosan Membranes as a Potential PEMFC Electrolyte. *Journal of Polymers and the Environment*, 2018, 26(7): p. 2964-2972. DOI: 10.1007/s10924-017-1146-7
- [19] Pillai, C. K. S., Paul, W., & Sharma, C. P. Chitin and chitosan polymers: Chemistry, solubility and fiber formation. *Progress in Polymer Science*, 2009, 34, 641–678. DOI:10.1016/j.progpolymsci.2009.04.001
- [20] Casadidio C, Peregrina DV, Gigliobianco MR, Deng S, Censi R, Di Martino P. Chitin and Chitosans: Characteristics, Eco-Friendly Processes, and Applications in Cosmetic Science. *Mar Drugs*. 2019 Jun 21; 17(6):369. doi: 10.3390/md17060369
- [21] Dassanayake, Rohan & Acharya, Sanjit & Abidi, Nouredine. *Biopolymer-Based Materials from Polysaccharides: Properties, Processing, Characterization and Sorption Applications*, (2018). DOI:10.5772/intechopen.80898
- [22] Domard, A. A perspective on 30 years research on chitin and chitosan. *Carbohydrate Polymers*, 2011, 84, 696–703. <https://doi.org/10.1016/j.carbpol.2010.04.083>
- [23] Rungnim, C., Ringrotmongkol, T., Hannongbua, S., & Okumura, H. Replica exchange molecular dynamics simulation of chitosan for drug delivery system based on carbon nanotube. *Journal of Molecular Graphics and Modelling*, 2013, 39, 183–192. DOI:10.1016/j.jmgm.2012.11.004
- [24] Zhu, H. Y., Fu, Y. Q., Jiang, R., Yao, J., Liu, L., & Zeng, G. M. Preparation, characterization and adsorption properties of chitosan modified magnetic graphitized multiwalled carbon nanotubes for highly effective removal of a carcinogenic dye from aqueous solution. *Applied Surface Science*, 2013, 285, 865–873. <https://doi.org/10.1016/j.apsusc.2013.09.003>
- [25] Dutta PK, Dutta J, Tripathi VS Chitin and chitosan: chemistry, properties and applications, *Journal of Scientific & Industrial Research*, 2004, 63, 20-31.
- [26] Bansal V, Sharma PK, Sharma N, Pal OP, Malviya R Applications of chitosan and chitosan derivatives in drug delivery. *Adv Biol Res* 2011, 5:28–37.
- [27] Corradini E, De Moura MR, Mattoso LHC, A preliminary study of the incorporation of NPK fertilizer into chitosan nanoparticles. *Express Polym Lett*, 2010, 4:509–515. DOI:10.3144/expresspolymlett.2010.64
- [28] Nur Fatin Ab. Rahman, Loh Kee Shyuan, Abu Bakar Mohamad, Abdul Amir H. Kadhum, “Review on Biopolymer Membranes for Fuel Cell Applications “ , *Applied Mechanics and Materials*, 2013, Vol. 291 pp. 614-617. <https://doi.org/10.4028/www.scientific.net/AMM.291-294.614>
- [29] Hafez, A., Chemical-modifications-of-chitosan-biopolymer-as-poly-electrolyte-membrane-for-full-cells-Article-review. *International Journal of Scientific & Engineering Research* Volume 11, 2020.
- [30] Ahmed, S.; Cai, Y.; Ali, M.; Khanal, S.; Xu, S. Preparation and performance of nanoparticle-reinforced chitosan proton-exchange membranes for fuel-cell applications. *J. Appl. Polym. Sci.*, 2018, 136. <https://doi.org/10.1002/app.46904>
- [31] Tsen, W. C. Composite proton exchange membranes based on chitosan and phosphotungstic acid immobilized one-dimensional attapulgite for direct methanol fuel cells, *Nanomaterials*, 2020, 10, 1641. <https://doi.org/10.3390/nano10091641>
- [32] Shen, S.; Jia, T.; Jia, J.; Wang, N.; Song, D.; Zhao, J.; Jin, J.; Che, Q. Constructing anhydrous proton exchange membranes through alternate

- depositing graphene oxide and chitosan on sulfonated poly (vinylidene fluoride) or sulfonated poly (vinylidene fluoride-co-hexafluoropropylene) membranes. *Eur. Polym. J.* 2021, 142, 110160. <https://doi.org/10.1016/j.eurpolymj.2020.110160>
- [33] Ahmed S, Ikram S Chitosan & its derivatives: a review in recent innovations. *Int J Pharma Sci Res*, 2015, 6:14–30. [DOI:10.13040/IJPSR.0975-8232.6\(1\).14-30](https://doi.org/10.13040/IJPSR.0975-8232.6(1).14-30)
- [34] Picos-Corrales, L.A.; Morales-Burgos, A.M.; Ruelas-Leyva, J.P.; Crini, G.; García-Armenta, E.; Jimenez-Lam, S.A.; Ayón-Reyna, L.E.; Rocha-Alonzo, F.; Calderón-Zamora, L.; Osuna-Martínez, U.; et al. Chitosan as an Outstanding Polysaccharide Improving Health-Commodities of Humans and Environmental Protection. *Polymers*, 2023, 15, 526. <https://doi.org/10.3390/polym15030526>
- [35] Thambiliyagodage, C.; Jayanetti, M.; Mendis, A.; Ekanayake, G.; Liyanaarachchi, H.; Vigneswaran, S. Recent Advances in Chitosan-Based Applications—A Review. *Materials* 2023, 16, 2073. <https://doi.org/10.3390/ma16052073>
- [36] Murat Yanat, Karin Schroën, Preparation methods and applications of chitosan nanoparticles; with an outlook toward reinforcement of biodegradable packaging, *Reactive and Functional Polymers*, Volume 161, 2021, 104849. <https://doi.org/10.1016/j.reactfunctpolym.2021.104849>
- [37] Mohammed MA, Syeda JTM, Wasan KM, Wasan EK. An Overview of Chitosan Nanoparticles and Its Application in Non-Parenteral Drug Delivery. *Pharmaceutics*. 2017 Nov 20; 9(4):53. [doi: 10.3390/pharmaceutics9040053](https://doi.org/10.3390/pharmaceutics9040053)
- [38] Dimassi, Syrine; Tabary, Nicolas; Chai, Feng; Blanchemain, Nicolas; Martel, Bernard. SULFONATED AND SULFATED CHITOSAN DERIVATIVES FOR BIOMEDICAL APPLICATIONS: A REVIEW, *Carbohydrate Polymers*, 2018, (18). [DOI: 10.1016/j.carbpol.2018.09.011](https://doi.org/10.1016/j.carbpol.2018.09.011)
- [39] Ma, J., & Sahai, Y. Chitosan biopolymer for fuel cell applications. *Carbohydrate Polymers*, 2013, 92, 955–975. [DOI: 10.1016/j.carbpol.2012.10.015](https://doi.org/10.1016/j.carbpol.2012.10.015)
- [40] Marroquin, J. B., Rhee, K. Y., & Park, S. J. Chitosan nanocomposite films: Enhanced electrical conductivity, thermal stability, and mechanical properties. *Carbohydrate Polymers*, 2013, 92, 1783–1791. [DOI: 10.1016/j.carbpol.2012.11.042](https://doi.org/10.1016/j.carbpol.2012.11.042)
- [41] Yang, J. M., & Chiu, H. C. Preparation and characterization of polyvinyl alcohol/chitosan blended membrane for alkaline direct methanol fuel cells. *Journal of Membrane Science*, 2012, 419–420, 65–71. [DOI:10.1016/j.memsci.2012.06.051](https://doi.org/10.1016/j.memsci.2012.06.051)
- [42] Tripathi, B. P., & Shahi, V. K. Organic–inorganic nanocomposite polymer electrolyte membranes for fuel cell applications. *Progress in Polymer Science*, 2011, 36, 945–979. <https://doi.org/10.1016/j.progpolymsci.2010.12.005>
- [43] Vijayakumar, V.; Nam, S.Y. A Review of Recent Chitosan Anion Exchange Membranes for Polymer Electrolyte Membrane Fuel Cells. *Membranes* 2022, 12, 1265. <https://doi.org/10.3390/membranes12121265>
- [44] Tsen WC. Composite Proton Exchange Membranes Based on Chitosan and Phosphotungstic Acid Immobilized One-Dimensional Attapulgite for Direct Methanol Fuel Cells, *Nanomaterials (Basel)*, 2020 Aug 21;10(9):1641. <https://doi.org/10.3390/nano10091641>
- [45] Rosli NAH, Loh KS, Wong WY, Lee TK, Ahmad A., Hybrid Composite Membrane of Phosphorylated Chitosan/Poly (Vinyl Alcohol)/Silica as a Proton Exchange Membrane, *Membranes (Basel)*. 2021 Aug 31; 11(9):675. [DOI:10.3390/membranes11090675](https://doi.org/10.3390/membranes11090675)
- [46] R. Jayakumar, N. Nwe, S. Tokura, & H. Tamura, “Sulfated Chitin and Chitosan as novel biomaterials” *International J. of biological Macromolecules*, 2007, Vol.40, pp. 175-181. [DOI: 10.1016/j.ijbiomac.2006.06.021](https://doi.org/10.1016/j.ijbiomac.2006.06.021)
- [47] Harish Prashanth, K. V., & Tharanathan, R. N. “Chitin/chitosan: Modifications and their unlimited application potential - An overview”. *Trends in Food Science & Technology*, 2007, Vol. 18, pp. 117–131. <https://doi.org/10.1016/j.tifs.2006.10.022>
- [48] Siti Wafiroh, Abdulloh, Winda Kusuma Wardani “Production and characterization of sulfonated chitosan-Calcium Oxide composite membrane as a proton exchange fuel cell membrane” *Journal of Chemical Technology and Metallurgy*, 2017, Vol. 6, pp. 1092-1096.
- [49] Bagaskara, Muharom & Azizah, A & Ni'mah, A & Hapsari, P & Saputra, Ozi & Dewi, C & Pramono, Edi. New route for synthesis and characterization sulfonated chitosan using acetyl sulfate as a sulfonating agent. *Journal of Physics: Conference Series*, 2022 2190(1):012023. [DOI:10.1088/1742-6596/2190/1/012023](https://doi.org/10.1088/1742-6596/2190/1/012023)
- [50] S. Sabar, H. Abdul Aziz, N.H. Yusof, S. Subramaniam, K.Y. Foo, L.D. Wilson, H.K. Lee,

- Preparation of sulfonated chitosan for enhanced adsorption of methylene blue from aqueous solution, *Reactive and Functional Polymers*, 2020, Volume 151. [DOI:10.1016/j.reactfunctpolym.2020.104584](https://doi.org/10.1016/j.reactfunctpolym.2020.104584)
- [51] Zhang, X. and J. Sun, Synthesis, Characterization, and Properties of Sulfonated Chitosan for Protein Adsorption. *International Journal of Polymer Science*, 2020, p. 1-10. <https://doi.org/10.1155/2020/9876408>
- [52] Tang, C.L., A Novel Solid-acid Catalyst Using Sulfonated Crosslinked Chitosan Resin. *Chemical and Biochemical Engineering Quarterly*, 2016, 30(2): p. 227-236. <http://dx.doi.org/10.15255/CABEQ.2015.2279>
- [53] Kavianinia, I., Plieger, P.G., Kandile, N.G. and Harding, D.R., Preparation and characterization of chitosan films, crosslinked with symmetric aromatic dianhydrides to achieve enhanced thermal properties. *Polym. Int.*, 2015, 64: 556-562. <https://doi.org/10.1002/pi.4835>
- [54] Mukoma, B.R. Jooste, H.C.M. Vosloo. Synthesis and characterization of cross-linked chitosan membranes for application as alternative proton exchange membrane materials in fuel cells. *Journal of Power Sources* 2004, 136, 16–23 P. <https://doi.org/10.1016/j.jpowsour.2004.05.027>
- [55] Paturzo, L Basile, A., Iulianelli, A., Jansen, J. C., Gatto, I., and Passalacqua, E High temperature proton exchange fuel cell using a sulphonated membrane obtained via H<sub>2</sub>SO<sub>4</sub> treatment of PEEK-WC, *Journal Catalysis Today*, 2005, 104: 213-218. [DOI:10.1016/j.cattod.2005.03.050](https://doi.org/10.1016/j.cattod.2005.03.050)
- [56] Bebin, P., Caravanier, M and Galiano, H. Nafion®/Clay –SO<sub>3</sub>H membrane for proton exchange membrane fuel cell application, *Journal of Membrane Science*, 2005, 278: 35- 42. [doi:10.1016/j.memsci.2005.10.042](https://doi.org/10.1016/j.memsci.2005.10.042)
- [57] Ahmed, S., et al., Preparation and Characterization of a Novel Sulfonated Titanium Oxide Incorporated Chitosan Nanocomposite Membranes for Fuel Cell Application. *Membranes*, 2021. 11(6): p. 450. <https://doi.org/10.3390/membranes11060450>
- [58] Mokrini, A., Huneault, M. A and Gerard, P. Partially fluorinated proton exchange membranes based on PVDF-SEBS blends compatibilized with methylmethacrylate block copolymers. *Journal of Membrane Science*, 2006, 283: 74-83. <https://doi.org/10.1016/j.memsci.2006.06.032>
- [59] Larminie, J and Dicks, A. Fuel cell systems explained. John Wiley & Sons, Ltd, England, 2000, pp 1-50.
- [60] Tamer, T.M., et al., Development of polyelectrolyte sulphonated chitosan-alginate as an alternative methanol fuel cell membrane. *Desalination and Water Treatment*, 2021. 227: p. 132-148. [DOI:10.5004/dwt.2021.27290](https://doi.org/10.5004/dwt.2021.27290)
- [61] Daoust, D., Devaux, J and Godard, P. Mechanism and kinetics of poly(ether ether ketone) (PEEK) sulphonation in concentrated sulphuric acid at room temperature, Part 1, Quantitative comparison between polymer and monomer model compound sulphonation. *Polymer International*, 2001, 50: 917-924. <https://doi.org/10.1002/pi.720>
- [62] Nobuhiro, S and Roger, S. P. A reconsideration of the kinetics of aromatic sulphonation by sulphuric acid. *Macromolecules*, 1994, 27: 6267-6271. [DOI:10.1021/MA00100A006](https://doi.org/10.1021/MA00100A006)
- [63] Smitha, B., Sridhar, S., Khan, A. A. Synthesis and characterization of proton conducting polymer membranes for fuel cells, *Journal Membrane Science*, 2003, 225: 63-76. [DOI:10.1016/S0376-7388\(03\)00343-0](https://doi.org/10.1016/S0376-7388(03)00343-0)
- [64] Zongwu, B, Michael, F. D., and Thuy, D. D. Proton conductivity and properties of sulfonated polyarylenethioether sulfones as proton exchange membranes in fuel cells. *Journal of Membrane Science*, 2006, 281: 508-516. <https://doi.org/10.1016/j.memsci.2006.04.021>
- [65] Christopher Avwoghokoghene, PhD Sulfonation of synthetic rubber as an alternative membrane for proton exchange membrane fuel cell, PhD Johansbur, 9,2009.
- [66] Sigwadi, R., et al., Nafion®/ sulfated zirconia oxide-nanocomposite membrane: the effects of ammonia sulfate on fuel permeability. *Journal of Polymer Research*, 2019, 26(5). <http://dx.doi.org/10.1007/s10965-019-1760-2>